

Building and evaluation of a PBPK model for S-Mephenytoin in adults

Version	1.1-OSP11.2
based on <i>Model Snapshot and Evaluation Plan</i>	https://github.com/Open-Systems-Pharmacology/S-Mephenytoin-Model/releases/tag/v1.1
OSP Version	11.2
Qualification Framework Version	2.3

This evaluation report and the corresponding PK-Sim project file are filed at:

<https://github.com/Open-Systems-Pharmacology/OSP-PBPK-Model-Library/>

Table of Contents

- 1 Introduction
- 2 Methods
 - 2.1 Modeling Strategy
 - 2.2 Data
 - 2.3 Model Parameters and Assumptions
- 3 Results and Discussion
 - 3.1 Final input parameters
 - 3.2 Diagnostics Plots
 - 3.3 Concentration-Time Profiles
 - 3.3.1 Model Verification
- 4 Conclusion
- 5 References
- 6 Glossary

1 Introduction

The presented PBPK model of S-mephenytoin has been developed to be used in a PBPK Drug-Drug-Interactions (DDI) network with S-mephenytoin as a substrate of CYP2C19.

Mephenytoin is a hydantoin-derivative anticonvulsant used to control various partial seizures and was first used in the 1940s ([Troupin 1979](#)).

Only limited clinical PK and ADME data are available. Mephenytoin is soluble and rapidly absorbed with a T_{max} of 1 hour. The mean half-life in human is 6.8 hours. No hints for dose non-linearity could be found in literature.

Mephenytoin is the mixture of the two enantiomers S- and R-Mephenytoin. S-Mephenytoin is mainly metabolized via CYP2C19. Only a very minor part is metabolized by CYP2C9. The R-enantiomer is not metabolized by CYP2C19. The clearance of S-Mephenytoin in CYP2C19 EM is 40 to 100-fold higher than in PM.

2 Methods

2.1 Modeling Strategy

The general workflow for building an adult PBPK model has been described by Kuepfer et al. ([Kuepfer 2016](#)). Relevant information on the anthropometry (height, weight) was gathered from the respective clinical study, if reported. Information on physiological parameters (e.g. blood flows, organ volumes, hematocrit) in adults was gathered from the literature and has been incorporated in PK-Sim® as described previously ([Willmann 2007](#)). The applied activity and variability of plasma proteins and active processes that are integrated into PK-Sim® are described in the publicly available 'PK-Sim® Ontogeny Database Version 7.3' ([PK-Sim Ontogeny Database Version 7.3](#)).

Only the S-enantiomer of mephénytoin is modeled. The modeling work flow can be summarized as following:

Modelling step	Data used / comment
1.) Development of mean po model (no i.v. data available)	IVIVE based on physico-chemistry and in vitro metabolization or recalculated in vivo clearance. Alternative middle out fits to in vivo data were tried but could not improve DDI prediction significantly. Additional limited data lead to identifiability problems.
2.) Evaluation of p.o. model with virtual PK-Sim population	Range and mean plasma profiles after p.o. administration for the study population was in line with the PK-Sim in-built variability of CYP2C9 and CYP2C19.

The predefined “Standard European Male for DDI” individual was used (age = 30 y, weight = 73 kg, height = 176 cm, BMI = 23.57 kg/m²). CYP2C19 expression from the PK-Sim in-built RT-PCR database was added.

Due to the limited data, an IVIVE approach has been selected. Parameters describing intrinsic CYP2C19 clearance were recalculated from CL/F ([Adedoyin 1998](#)) and in vitro metabolism data from human microsomes CYP2C19 clearance and CYP2C9 clearance ([Steere 2015](#)).

A simulation of a population with 2000 virtual individuals according to the biometrics of the individuals (8 males and females, 32-78 years) used in a study by [Adedoyin 1998](#) was carried out. Additional variability was included on CYP2C19 among the population, by using the geometric SD as derived from reported CL/F values in [Oliveras-Morales 2016](#).

Details about input data (physicochemical, *in vitro* and clinical) can be found in [Section 2.2](#).

Details about the structural model and its parameters can be found in [Section 2.3](#).

2.2 Data

2.2.1 In vitro and physico-chemical data

A literature search was performed to collect available information on physico-chemical properties of S-mephénytoin ([Table 1](#)).

Parameter	Unit	Value	Source	Description
MW ⁺	g/mol	218.52	DrugBank DB00532	Molecular weight.
pK _{a,acid} ⁺		8.51	DrugBank DB00532	Acidic dissociation constant
Solubility (pH) ⁺	mg/mL	1.27 (7)	DrugBank DB00532	Aqueous Solubility
logP ⁺		1.69	DrugBank DB00532	Partition coefficient
fu ⁺	%	70.2	Steere 2015	Fraction unbound in plasma

Table 1: Physico-chemical and *in-vitro* metabolization properties of S-mephenytoin extracted from literature. ⁺: Value used in final model

2.2.2 Clinical data

A literature search was performed to collect available clinical data on S-mephenytoin. Data used for model development and validation are listed in [Table 2](#).

Source	Route	Dose [mg]/ Schedule	Pop.	Age [yrs] (mean) /range	Weight [kg] (mean) /range	Sex	N	Form.	Comment
Adedoyin 1998	p.o.	100 mg s.d.	HV, all EM	54.7 / 32-73	-	m/f	8	tablet	50 g S-mephenytoin simulated
Jacqz 1986	p.o.	100 mg s.d.	HV, 6 EM, 1 IM and 1 PM	25-76	-	m/f	8	tablet	50 g S-mephenytoin simulated
Yao 2003	p.o.	100 mg s.d.	HV	23-49	-	m/f	12	-	S-mephenytoin, with and without Fluvoxamine MD of 37.5, 62.5 and 87.5 mg/day
Iga 2016	p.o.	100 mg s.d.	-	-	-	-	-	-	50 g S-mephenytoin simulated
Wedlund 1985	p.o.	100 mg s.d.	HV	21-7	54-108	male	8	tablet	50 g S-mephenytoin simulated

Table 2: Literature sources of clinical concentration data of S-mephenytoin used for model development and validation. *s.d.*: single dose

2.3 Model Parameters and Assumptions

2.3.1 Absorption

Intestinal permeability is calculated by PK-Sim. No data are available to estimate the parameter.

2.3.2 Distribution

Partition coefficient calculation by [Rodgers and Rowland](#) and cellular permeability calculation by [PK-Sim Standard](#) have been assumed. Identification of the best suited calculation methods was not possible due to lack of i.v. data.

2.3.3 Metabolism and Elimination

Two linear metabolic pathways for S-mephenytoin were implemented in the model:

- CYP2C19
- CYP2C9

Additionally, glomerular filtration was implemented with assumed GFR fraction of 1. No active renal excretion described in literature. Renal clearance is minor compared to overall plasma clearance ([Jacqz 1986](#)) and can be described by glomerular filtration.

2.3.5 Automated Parameter Identification

Performing parameter identification on lipophilicity, CYP2C19 intrinsic clearance, and intestinal permeability did not improve the performance of the model. Therefore, no parameters have been estimated.

3 Results and Discussion

The next sections show:

1. Final model input parameters for the building blocks: [Section 3.1](#).
2. Overall goodness of fit: [Section 3.2](#).
3. Simulated vs. observed concentration-time profiles for the clinical studies used for model building and for model verification: [Section 3.3](#).

3.1 Final input parameters

The parameter values of the final PBPK model are illustrated below.

Compound: S-Mephenytoin

Parameters

Name	Value	Value Origin	Alternative	Default
Solubility at reference pH	1.27 mg/ml	Database-DrugBank DB00532	Measurement	True
Reference pH	7	Database-DrugBank DB00532	Measurement	True
Lipophilicity	1.69 Log Units	Database-DrugBank DB00532	Measurement	True
Fraction unbound (plasma, reference value)	70.2 %	Publication-Steere 2015	Measurement	True
Is small molecule	Yes			
Molecular weight	218.52 g/mol	Database-DrugBank DB00532		
Plasma protein binding partner	Albumin			

Calculation methods

Name	Value
Partition coefficients	Rodgers and Rowland
Cellular permeabilities	PK-Sim Standard

Processes

Metabolizing Enzyme: CYP2C19-Adedoyin1998_Table1_CL_F

Species: Human

Molecule: CYP2C19

Parameters

Name	Value	Value Origin
Intrinsic clearance	1986.9 ml/min	Publication-Adedoyin 1998

Metabolizing Enzyme: CYP2C9-Steere2015_Clint_CYP2C9_Table1

Molecule: CYP2C9

Parameters

Name	Value	Value Origin
In vitro CL for liver microsomes	0.39 $\mu\text{l}/\text{min}/\text{mg}$ mic. protein	Publication-Steere2015
Content of CYP proteins in liver microsomes	96 pmol/mg mic. protein	Publication-Rodrigues 1999

Systemic Process: Glomerular Filtration-Assumption

Species: Human

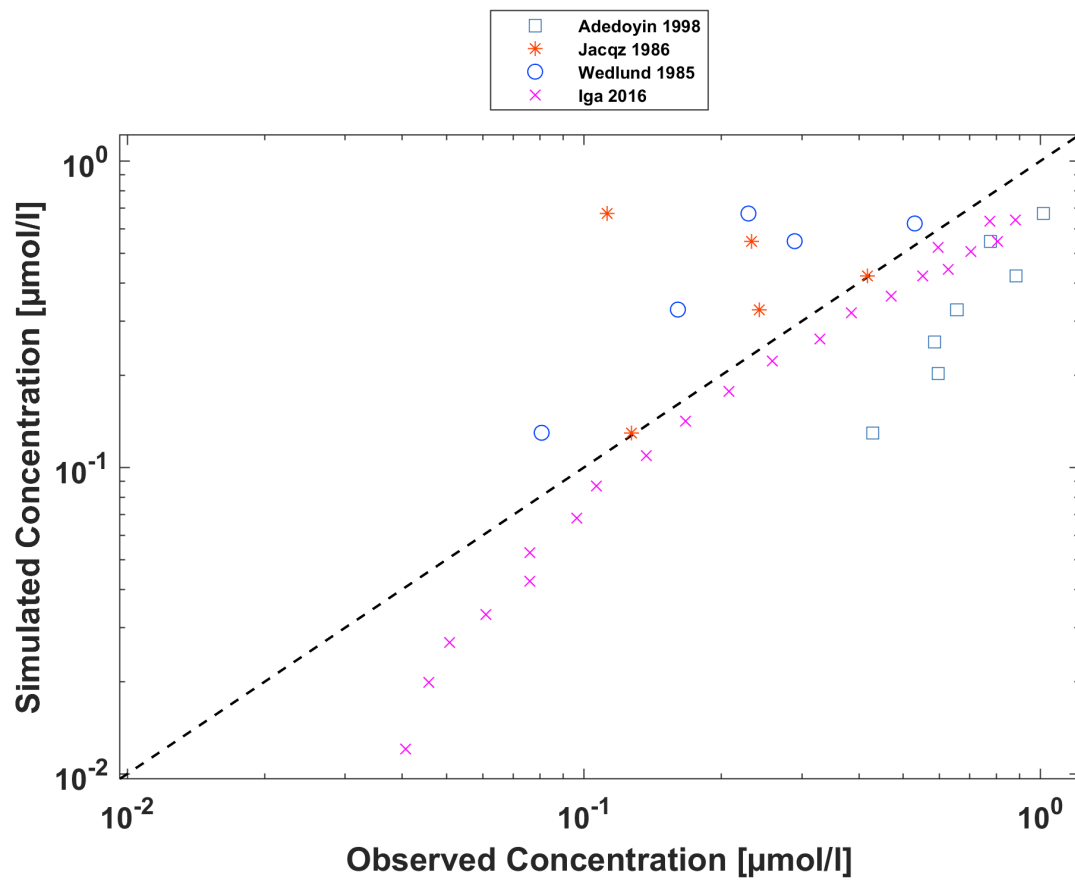
Parameters

Name	Value	Value Origin
GFR fraction	1	Other-Assumption

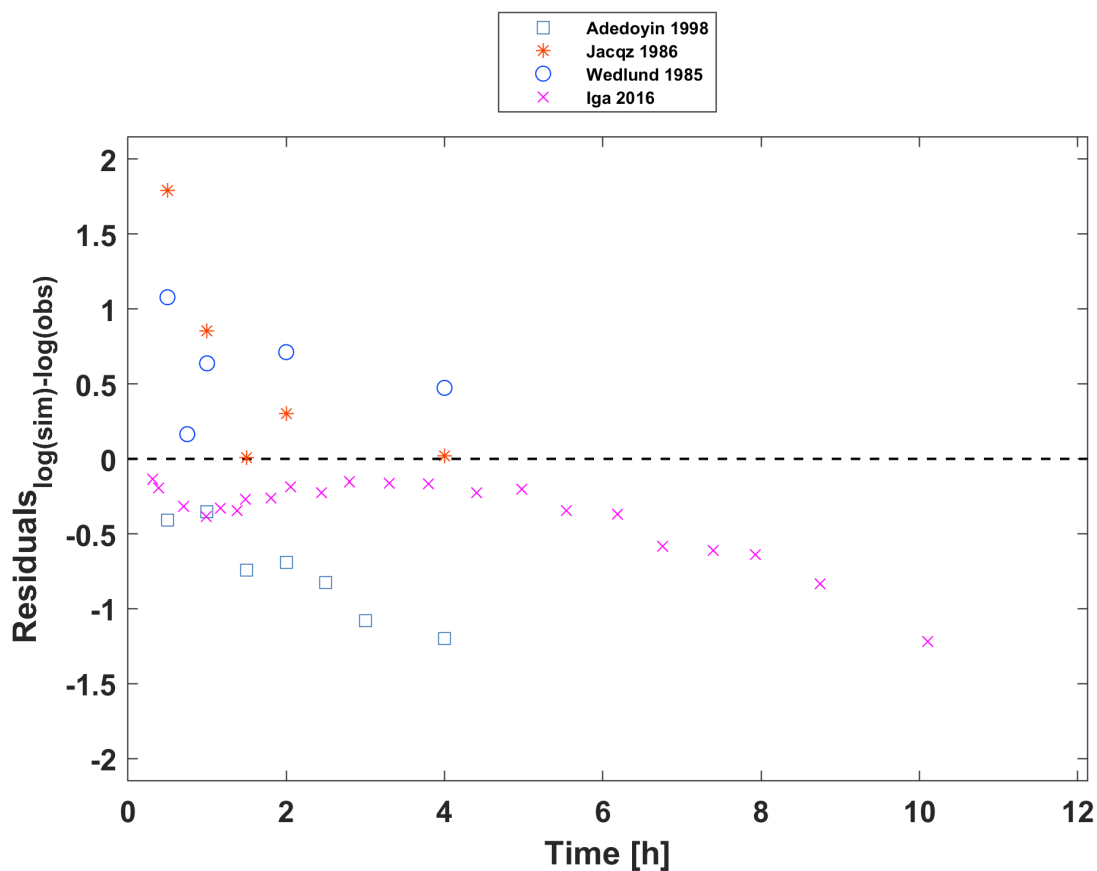
3.2 Diagnostics Plots

The following section displays the goodness-of-fit visual diagnostic plots for the PBPK model performance of all data listed in [Section 2.2.2](#).

The first plot shows observed versus simulated plasma concentration, the second weighted residuals versus time.



S-mephenytoin concentration in plasma after 50 mg oral administration - mean data



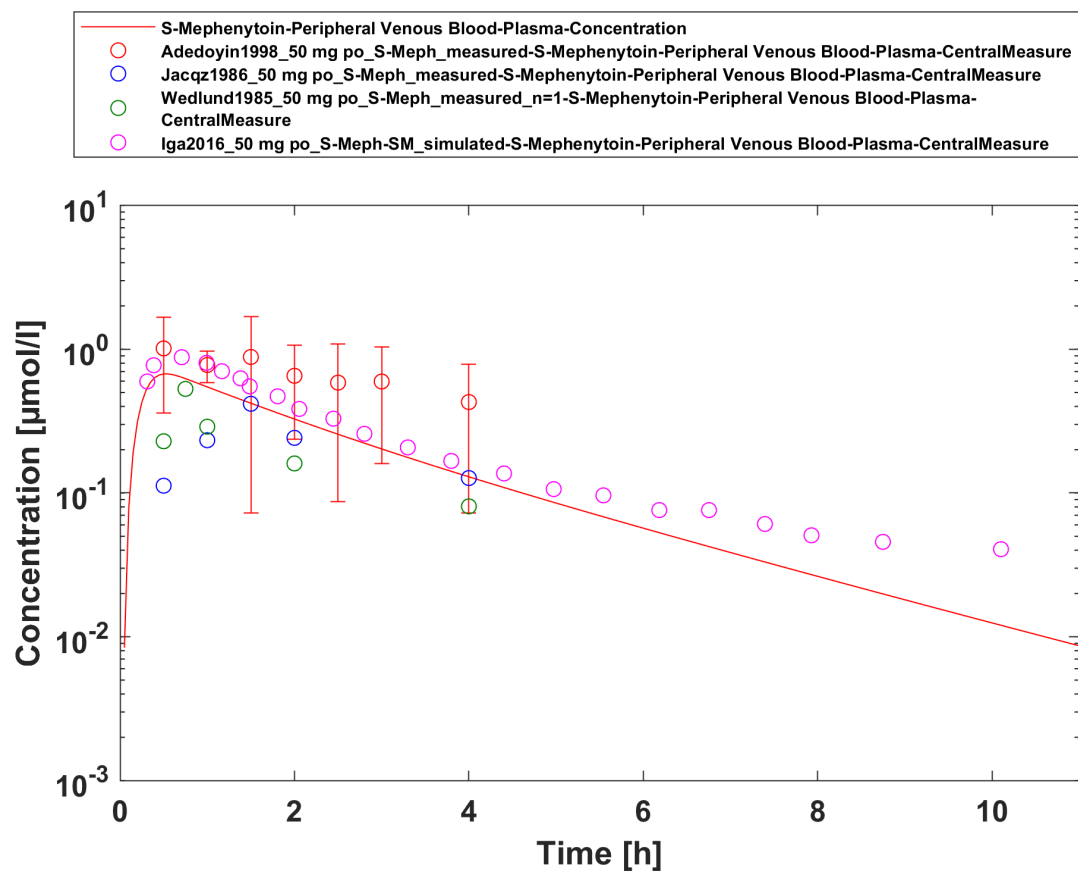
S-mephenytoin concentration in plasma after 50 mg oral administration - mean data

GMFE = 1.648579

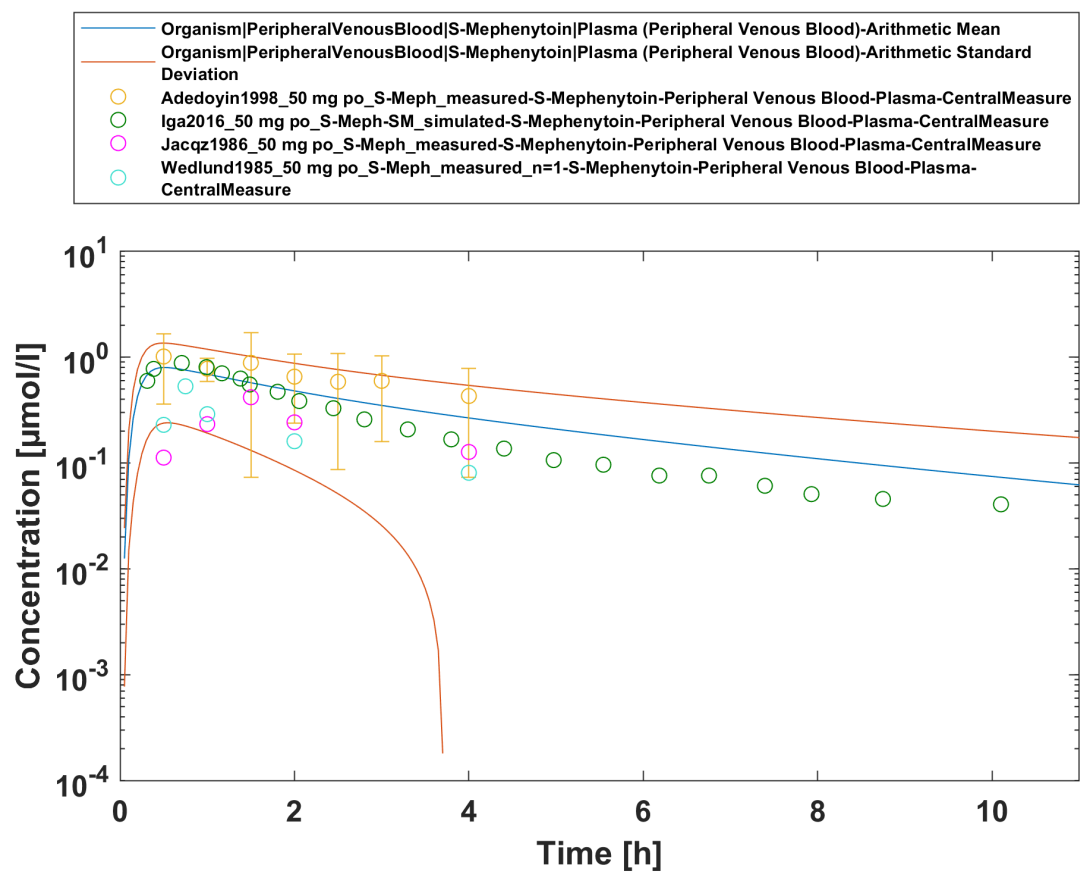
3.3 Concentration-Time Profiles

Simulated versus observed concentration-time profiles of all data listed in [Section 2.2.2](#) are presented below.

3.3.1 Model Verification



S-Mephenytoin 50 mg p.o.



Time Profile Analysis

4 Conclusion

A PBPK model describing the limited set of in vivo p.o. data could be established.

Population simulated data had a comparable variability with the observed data when included additional variability for CYP2C19 expression. Moreover, the mean data from other studies ([Jacqz 1986](#), [Wedlund 1985](#)) were in the range of expected variability, confirming the adequacy of the model.

5 References

Adedoyin 1998 Adedoyin A, Arns PA, Richards WO, Wilkinson GR, Branch RA. Selective effect of liver disease on the activities of specific metabolizing enzymes: investigation of cytochromes P450 2C19 and 2D6. *Clin Pharmacol Ther.* 1998;64(1):8-17.

DrugBank DB00532 (<https://www.drugbank.ca/drugs/DB00532>)

Iga 2016 Iga K. Dynamic and Static Simulations of Fluvoxamine-Perpetrated Drug-Drug Interactions Using Multiple Cytochrome P450 Inhibition Modeling, and Determination of Perpetrator-Specific CYP Isoform Inhibition Constants and Fractional CYP Isoform Contributions to Vic. *J Pharm Sci.* Victim Clearance. Journal of Pharmaceutical Sciences. 2016 Mar;105(3):1307-1317–17.

Jacqz 1986 Jacqz E, Hall SD, Branch RA, Wilkinson GR. Polymorphic metabolism of mephenytoin in man: Pharmacokinetic interaction with a co-regulated substrate, mephobarbital. *Clin Pharmacol Ther.* 1986;39(6):646-653.

Kuepfer 2016 Kuepfer L, Niederalt C, Wendl T, Schlender JF, Willmann S, Lippert J, Block M, Eissing T, Teutonico D. Applied Concepts in PBPK Modeling: How to Build a PBPK/PD Model. *CPT Pharmacometrics Syst Pharmacol.* 2016 Oct;5(10):516-531.

Olivares-Morales 2016 Olivares-Morales A, Ghosh A, Aarons L, Rostami-Hodjegan A. Development of a Novel Simplified PBPK Absorption Model to Explain the Higher Relative Bioavailability of the OROS(R) Formulation of Oxybutynin. *AAPS J.* 2016;18(6):1532-1549.

PK-Sim Ontogeny Database Version 7.3 (<https://github.com/Open-Systems-Pharmacology/OSPSuite.Documentation/blob/38cf71b384cfc25cfa0ce4d2f3addfd32757e13b/PK-Sim%20Ontogeny%20Database%20Version%207.3.pdf>)

Steere 2015 Steere B, Baker JAR, Hall SD, Guo Y. Prediction of in vivo clearance and associated variability of CYP2C19 substrates by genotypes in populations utilizing a pharmacogenetics-based mechanistic model. *Drug Metab Dispos.* 2015;43(6):870-883.

Troupin 1979 Troupin AS, Friel P, Lovely MP, Wilensky AJ. Clinical pharmacology of mephenytoin and ethotoin. *Ann Neurol.* 1979;6(5):410-414.

Wedlund 1985 Wedlund PJ, Aslanian WS, Jacqz E, McAllister CB, Branch RA, Wilkinson GR. Phenotypic differences in mephenytoin pharmacokinetics in normal subjects. *J Pharmacol Exp Ther.* 1985;234:662-669.

Willmann 2007 Willmann S, Höhn K, Edginton A, Sevestre M, Solodenko J, Weiss W, Lippert J, Schmitt W. Development of a physiology-based whole-body population model for assessing the influence of individual variability on the pharmacokinetics of drugs. *J Pharmacokinet Pharmacodyn* 2007, 34(3): 401-431.

Yao 2003 Yao C, Kunze KL, Trager WF, Kharasch ED, Levy RH. Comparison of in vitro and in vivo inhibition potencies of fluvoxamine toward CYP2C19. *Drug Metab Dispos.* 2003;31(5):565-571.

6 Glossary

ADME	Absorption, Distribution, Metabolism, Excretion
AUC	Area under the plasma concentration versus time curve
AUCinf	AUC until infinity
AUClast	AUC until last measurable sample
AUCR	Area under the plasma concentration versus time curve Ratio
b.i.d.	Twice daily (bis in diem)
CL	Clearance
Clint	Intrinsic liver clearance
Cmax	Maximum concentration
CmaxR	Maximum concentration Ratio
CYP	Cytochrome P450 oxidase
CYP1A2	Cytochrome P450 1A2 oxidase
CYP2C19	Cytochrome P450 2C19 oxidase
CYP3A4	Cytochrome P450 3A4 oxidase
DDI	Drug-drug interaction
e.c.	Enteric coated
EE	Ethinylestradiol
EM	Extensive metabolizers
fm	Fraction metabolized
FMO	Flavin-containing monooxygenase
fu	Fraction unbound
FDA	Food and Drug administration
GFR	Glomerular filtration rate
HLM	Human liver microsomes
hm	homozygous
ht	heterozygous
IM	Intermediate metabolizers
i.v.	Intravenous
IVIVE	In Vitro to In Vivo Extrapolation
Ka	Absorption rate constant
kcat	Catalyst rate constant
Ki	Inhibitor constant
Kinact	Rate of enzyme inactivation

ADME	Absorption, Distribution, Metabolism, Excretion
Km	Michaelis Menten constant
m.d.	Multiple dose
OSP	Open Systems Pharmacology
PBPK	Physiologically-based pharmacokinetics
PK	Pharmacokinetics
PI	Parameter identification
PM	Poor metabolizers
RT-PCR	Reverse transcription polymerase chain reaction
p.o.	Per os
q.d.	Once daily (quaque diem)
SD	Single Dose
SE	Standard error
s.d.SPC	Single dose Summary of Product Characteristics
SD	Standard deviation
TDI	Time dependent inhibition
t.i.d	Three times a day (ter in die)
UGT	Uridine 5'-diphospho-glucuronosyltransferase
UM	Ultra-rapid metabolizers